Inorg. Chem. **2006**, *45*, 1575–1584

Solvent Tuning of the Substitution Behavior of a Seven-Coordinate Iron(III) Complex

Ivana Ivanović-Burmazović,* Mohamed S. A. Hamza,† and Rudi van Eldik*

Institute for Inorganic Chemistry, University of Erlangen-Nürnberg, Egerlandstrasse 1, 91058 Erlangen, Germany

Received August 27, 2005

A detailed kinetic study of the substitution behavior of the seven-coordinate $[Fe(dapsox)(L)_2]ClO_4$ complex (H_2-dapsox = 2,6-diacetylpyridine-bis(semioxamazide), L = solvent or its deprotonated form) with thiocyanate as a function of the thiocyanate concentration, temperature, and pressure was undertaken in protic (EtOH and acidified EtOH and MeOH) and aprotic (DMSO) organic solvents. The lability and substitution mechanism depend strongly on the selected solvent (i.e., on solvolytic and protolytic processes). In the case of alcoholic solutions, substitution of both solvent molecules by thiocyanate could be observed, whereas in DMSO only one substitution step occurred. For both substitution steps, $[Fe(dapsox)(L)_2]ClO_4$ shows similar mechanistic behavior in methanol and ethanol, which is best reflected by the values of the activation volumes (MeOH $\Delta V^{\ddagger}_{I} = +15.0 \pm 0.3$ cm^3 mol^{-1}, $\Delta V^{\ddagger}_{II} = +12.0 \pm 0.2$ cm^3 mol^{-1}; EtOH $\Delta V^{\ddagger}_{I} = +15.8 \pm 0.7$ cm^3 mol^{-1}, $\Delta V^{\ddagger}_{II} = +11.1 \pm 0.5$ cm^3 mol^{-1}). On the basis of the reported activation parameters, a dissociative (D) mechanism for the first substitution step and a D or dissociative interchange (I_d) mechanism for the second substitution step are suggested for the reaction in MeOH and EtOH. This is consistent with the predominant existence of alcoxo [Fe(dapsox)(ROH)(OR)] species in alcoholic solutions. In comparison, the activation parameters for the substitution of the aqua-hydroxo $[Fe(dapsox)(H_2O)(OH)]$ complex by thiocyanate at pH 5.1 in MES were determined to be $\Delta H^{\ddagger} = 72 \pm 3$ kJ mol^{-1}, $\Delta S^{\ddagger} = +38 \pm 11$ J K^{-1} mol^{-1}, and $\Delta V^{\ddagger} = -3.0 \pm 0.1$ cm^3 mol^{-1}, and the operation of a dissociative interchange mechanism was suggested, taking the effect of pressure on the employed buffer into account. The addition of triflic acid to the alcoholic solutions ([HOTf] = 10^{-3} and 10^{-2} M to MeOH and EtOH, respectively) resulted in a drastic changeover in mechanism for the first substitution step, for which an associative interchange (I_a) mechanism is suggested, on the basis of the activation parameters obtained for both the forward and reverse reactions and the corresponding volume profile. The second substitution step remained to proceed through an I_d or D mechanism (acidified MeOH $\Delta V^{\ddagger}_{II} = +9.2 \pm 0.2$ cm^3 mol^{-1}; acidified EtOH $\Delta V^{\ddagger}_{II} = +10.2 \pm 0.2$ cm^3 mol^{-1}). The first substitution reaction in DMSO was found to be slowed by several orders of magnitude and to follow an associative interchange mechanism ($\Delta S^{\ddagger} = -50 \pm 9$ J K^{-1} mol^{-1}, $\Delta V^{\ddagger}_{I} = -1.0 \pm 0.5$ cm^3 mol^{-1}), making DMSO a suitable solvent for monitoring substitution processes that are extremely fast in aqueous solution.

Introduction

Seven-coordinate 3d metal complexes are considered to be quite unstable and kinetically labile species, and their solution chemistry is largely undefined. Since a few years it was shown that these species exhibit extremely interesting chemical properties and catalytic activity.[1−7] They can catalyze disproportionation of deleterious superoxide radicals, even faster than natural enzymes,[7] and therefore became a challenging research area.

* To whom correspondence should be addressed. E-mail: ivanabi@chem.bg.ac.yu (I.I.-B.), vaneldik@chemie.umi-erlangen.de (R.v.E.).

† On leave from the Department of Chemistry, Faculty of Science, Ain Shams University, Cairo, Egypt.

(1) Zhang, D.; Busch, D. H.; Lennon, P. L.; Weiss, R. H.; Neumann, W. L.; Riley, D. P. *Inorg. Chem.* **1998**, *37*, 956−963.
(2) Riley, D. P. *Chem. Rev.* **1999**, *99*, 2573−2587.
(3) Salvemini, D.; Wang, Z.; Zweier, J. L.; Samouilov, A.; Macarthur, H.; Misko, T. P.; Currie, M. G.; Cuzzocrea, S.; Sikorski, J. A.; Riley, D. P. *Science* **1999**, *286*, 304−306.
(4) Cabelli, D. E.; Riley, D.; Rodriguez, J. A.; Joan, S.; Zhu, H. *Biomimetic Oxidations Catalyzed by Transition Metal Complexes*; Meunier, B., Ed.; Imperial College Press: London, 2000; pp 461−508.
(5) Salvemini, D.; Riley, D. P.; Cuzzocrea, S. *Nat. Rev. Drug Discovery* **2002**, *1*, 367−374.

10.1021/ic0514694 CCC: $33.50
Published on Web 01/19/2006

Scheme 1

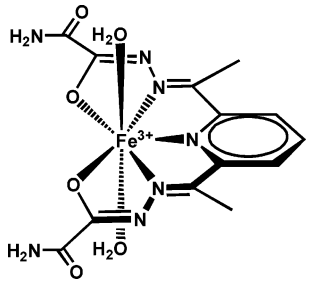

In the usual pentagonal-bipyramidal (PBP) structures of seven-coordinate complexes, the axial bonds are shorter than the equatorial ones. Thus, complexes with strongly chelating pentadentate ligands in the equatorial plane and more labile monodentate ligands in the axial positions can be very stable species and remain seven-coordinate even in solution.[8,9] The best SOD mimetics known to date are PBP complexes of Mn(II) with macrocyclic pentadentate ligands, pyridine derivatives of pentaazacyclopentadecane [15]aneN$_5$, in the equatorial plane, and Cl^- and H_2O as axial ligands in the solid state and in aqueous solution, respectively.[2,3,7] Iron SOD mimetics would also be desirable because of their generally higher stability than manganese complexes.[2] However, the Fe(III) complexes with [15]aneN$_5$-type macrocycles have quite low pK_a values for the coordinated water molecules[1] and have a tendency to react with the superoxide disproportionation product H_2O_2, which are serious drawbacks in terms of their catalytic activity under physiological conditions.[2]

We have systematically studied 3d metal complexes with the acyclic planar H_2dapsox pentadentate ligand and its deprotonated Hdapsox$^-$ and dapsox^{2-} forms (H_2dapsox = 2,6-diacetylpyridine-bis(semioxamazide)).[10] This ligand enables easy formation of the seven-coordinate metal geometry and forms a very stable PBP [Fe^{III}(dapsox)(H_2O)$_2$]ClO_4 complex (Scheme 1), despite of the acyclic nature of dapsox^{2-}. In our earlier work,[9] we focused on detailed mechanistic studies of the two-step substitution reaction of [Fe(dapsox)(H_2O)$_2$]ClO_4 with SCN^- (where SCN^- substitutes for the axially coordinated solvent molecules to produce [Fe(dapsox)(NCS)$_2$]$^-$) in aqueous solution, as a function of thiocyanate concentration, pH, temperature, and pressure. For a coordination number of 7, a high kinetic lability of the Fe(III) PBP complexes and the operation of a limiting dissociative mechanism are expected. However, specific structural and electronic properties of dapsox^{2-} resulted in an unexpected I_a mechanism for the seven-coordinate [Fe(dapsox)(H_2O)$_2$]$^+$ species.[9] The changeover in mechanism to I_d for substitution reactions of [Fe(dapsox)(H_2O)(OH)] and [Fe(dapsox)(NCS)(H_2O)] is caused by the electroneutrality of these complexes and the trans labilizing effect of coordinated OH^- and SCN^-, respectively. It was also shown[9] that the acyclic dapsox^{2-} ligand has specific electronic properties that cause a decrease in the acidity of the coordinated water molecules and produce a maximum concentration of aqua-hydroxo species at a physiological pH. The aqua-hydroxo complex is more than 500 times more reactive than the corresponding diaqua form.[9] This, together with the high stability, appropriate redox potential and high reaction selectivity toward superoxide, are important features of [Fe(dapsox)(H_2O)(OH)]ClO_4 in terms of its potential SOD activity.[11] This results from the fact that the first and rate-determining step in the SOD catalytic cycle of seven-coordinate Fe(III) mimetics is proposed to be substitution of the coordinated water molecule by $O_2^{\bullet -}$ in a dissociative manner.[1] In this context, the solution chemistry of [Fe(dapsox)(H_2O)$_2$]ClO_4 continued to attract our attention. Seven-coordinate complexes are not only important as excellent catalysts for superoxide disproportionation; they also show a general potential for being interesting redox active compounds. Since the solution properties and mechanistic behavior of seven-coordinate 3d metal complexes are still unrevealed research areas, studies which lead to the understanding of their structure−reactivity relationships are of fundamental importance.

The work presented here focuses on the clarification of the behavior, reactivity, ligand substitution mechanism, and protolytic processes of [Fe(dapsox)(H_2O)$_2$]ClO_4 in different solvents. We have now determined activation parameters for the substitution reaction of the aqua-hydroxo [Fe(dapsox)(H_2O)(OH)] complex with SCN^-, for which we had previously[9] determined rate constants and postulated a possible mechanism. We have studied the substitution behavior of [Fe(dapsox)(H_2O)$_2$]ClO_4 in MeOH solution before,[12] and the results indicated that the predominant complex species in solution is [Fe(dapsox)(MeOH)(OMe)], which is the reason for the operation of a dissociative mechanism. We have now extended the work to EtOH, acidified MeOH and EtOH solutions, and DMSO. These solvents were selected because kinetic experiments with the superoxide radical anion, especially with more concentrated solutions (in the millimolar range) presently in progress, require the use of aprotic solvents (usually DMSO or DMSO/CH_3CN mixtures), and the mixing of such KO_2 solutions with aqueous or alcoholic complex solutions for kinetic measurements at ambient or low temperatures, respectively.

Experimental Section

Materials. All solid chemicals were of p.a. grade and used as received without any further purification. For the kinetic measurements, p.a. grade ethanol, methanol, and DMSO were purchased

(6) Muscoli, C.; Cuzzocrea, S.; Riley, D. P.; Zweier, J. L.; Thiemermann, C.; Wang, Z.-Q.; Salvemini, D. *Br. J. Pharmacol.* **2003**, *140*, 445−460.
(7) Aston, K.; Rath, N.; Nauk, A.; Slomczynska, U.; Schall, O. F.; Riley, D. P. *Inorg. Chem.* **2001**, *40*, 1779−1789.
(8) Riley, D. P.; Henke, S. L.; Lennon, P. J.; Weiss, R. H.; Neumann, W. L.; Rivers, W. J., Jr.; Aston, K. W.; Sample, K. R.; Rahman, H.; Ling, C.-S.; Shieh, J.-J.; Busch, D. H.; Szulbinski, W. *Inorg. Chem.* **1996**, *35*, 5213−5231.
(9) Ivanović-Burmazović, I.; Hamza, M. S. A.; van Eldik, R. *Inorg. Chem.* **2002**, *41*, 5150−5161.
(10) Ivanović-Burmazović, I.; Andjelkovic, K. *Adv. Inorg. Chem.* **2004**, *55*, 315−360.
(11) Ivanović-Burmazović, I.; Liu, G.-F.; Heinemann, F.; van Eldik, R. in preparation.
(12) Ivanović-Burmazović, I.; Hamza, M. S. A.; van Eldik, R. *Inorg. Chem. Commun.* **2002**, *5*, 937−940.

from Merck and used without further drying. Test measurements showed that small quantities of water present in commercially available ethanol, methanol, and DMSO did not affect the kinetic measurements. $[Fe(dapsox)(H_2O)_2]ClO_4$ was prepared and characterized as described before.[10,13]

Instrumentation and Measurements. IR spectra were recorded on a Mattson FTIR Infinity spectrophotometer using KBr pellets, as well as a KBr cell for samples in DMSO and DMSO/H_2O solutions. UV−vis spectra were recorded on Shimadzu UV-2101 and Hewlett-Packard 8542A spectrophotometers.

Kinetic data were obtained by recording time-resolved UV−vis spectra using a modified Bio-Logic stopped-flow module μSFM-20 combined with a Huber CC90 thermostat and equipped with a J & M TIDAS high-speed diode array spectrometer with combined deuterium and tungsten lamps (200−1015 nm wavelength range). Isolast O-rings were used for all sealing purposes to allow measurements in DMSO. Data were analyzed using the integrated Bio-Kine software, version 4.23, and the Specfit/32 program. At least 10 kinetic runs were recorded under all conditions, and the reported rate constants represent the mean values. All kinetic measurements were carried out under pseudo-first-order conditions; i.e., the ligand concentration was in a large excess (complex concentration 5×10^{-5} M). The reactions were studied at an ionic strength of 0.3 M (LiOTf). Measurements under high pressure were carried out using a homemade high-pressure stopped-flow instrument,[14] for which Isolast O-rings were also used for all syringe seals.

The UV−vis spectrophotometers and stopped-flow instruments were thermostated to the desired temperature ±0.1 °C. Values of $\Delta H^{\ddagger}$ and $\Delta S^{\ddagger}$ were calculated from the slopes and intercepts of plots of $\ln(k/T)$ versus $1/T$, respectively, and values of $\Delta V^{\ddagger}$ were calculated from the slope of plots of $\ln(k)$ versus pressure in the usual manner.

The pK_a values of $[Fe(dapsox)(H_2O)_2]ClO_4$ at 0.5 °C were obtained by standard potentiometric titration on a METROHM 702 SM Titrino, and the data were fitted by Titfit.[15]

Equilibrium Measurements. Solutions of $[Fe(dapsox)(H_2O)_2]ClO_4$ (5×10^{-5} M) were prepared in acidified alcohol ([HOTf] = 10^{-3} M in MeOH and 10^{-2} M in EtOH) and DMSO, and they were placed in a 1.0 cm path length cuvette in the thermostated cell block of a spectrophotometer for 20 to 30 min. This solution was titrated by the addition of small volumes of a concentrated stock solution of sodium thiocyanate in acidified alcohols and DMSO, respectively, using a Hamilton glass syringe. In the alcohol solutions, higher thiocyanate concentrations were obtained by addition of solid NaSCN. The spectra were recorded 10 to 30 min after the addition of thiocyanate. The titrations were carried out in duplicate and were monitored in the 350−700 nm wavelength range. Estimation of the binding constants, K_1 and K_2, in acidified alcohol solutions was performed with the software package Specfit/32 global analysis and by fitting the absorbance versus concentration plot (after correction for dilution) at the wavelength where the largest change in absorbance occurred.

It should be pointed out that for DMSO solutions only glass equipment and Hamilton Teflon valves can be used!

Results and Discussion

Reaction of the Aqua-Hydroxo Complex. Previously,[9] we determined the activation parameters for the first step of the reaction between the diaqua $[Fe(dapsox)(H_2O)_2]^+$ species and SCN^- working at pH 2.5, and these are in agreement with the operation of an I_a mechanism. In this study, we have now determined the activation parameters for the reaction between the complex and SCN^- at pH 5.1 and, thereby, focused only on the first reaction step to verify the proposed substitution mechanism for $[Fe(dapsox)(H_2O)(OH)]$. The second reaction step, which can also be observed under selected experimental conditions, was studied before.[9] A detailed reaction scheme that includes all acid−base equilibria present in aqueous solution, has also been reported.[9] This pH value was selected since, at higher pH, the reaction became too fast to be followed by temperature- and pressure-dependent stopped-flow measurements. At the same time, since the aqua-hydroxo complex is ca. 500 times more reactive than the diaqua complex at pH 5.1 (although it is not very close to the pK_{a1} value of $[Fe(dapsox)(H_2O)_2]^+$, which was found to be 5.78 at 25 °C[9] and 6.02 at 0.5 °C), the kinetic contribution of the $[Fe(dapsox)(H_2O)(OH)]$ species (k_b) to the overall k_{obs} value is predominant. Therefore, k_{obs} was measured as function of temperature and pressure (Table S1, Supporting Information) at pH 5.1 in the presence of 0.1 M MES buffer and $[SCN^-] = 1$ M. The effect of temperature on the pK_a values of the selected buffer was found to be negligible, and the pressure effect was quite small (viz., $\Delta V(K_a) = +3.9 \pm 0.1$ cm^3 mol^{-1}).[16] The experiment was also repeated using piperazin as a buffer which has a higher buffer capacity at pH 5.1 than MES buffer but with a somewhat more positive value of $\Delta V(K_a)$ (+6.2 cm^3 mol^{-1}).[17] Plots of ln k_{obs} versus pressure gave a good linear fit in both cases, from which the apparent $\Delta V^{\ddagger}$ values were found to be -3.0 ± 0.1 and -3.8 ± 0.1 cm^3 mol^{-1} for the measurements in the MES and piperazin buffers, respectively. Since under the selected conditions $k_{obs} \approx k_b K_{a1}/(K_{a1} + [H^+])$,[9] the effect of pressure on the buffer and on the K_{a1} of the complex should be taken into account. The pressure effect on K_{a1} is expected to be small since upon proton dissociation of $[Fe(dapsox)(H_2O)_2]^+$ there is no change in overall charge. The only difference is that the charge is localized on a small proton instead of on the large complex cation upon dissociation, which can result in a small negative value of $\Delta V(K_{a1})$. Similar results have been found for various weak acids where there is also no charge creation upon dissociation.[16] Thus, taking this into consideration together with the above-mentioned pressure effect on the pK_a values of MES and piperazin, the value of $\Delta V^{\ddagger}(k_b)$ is expected to be small and positive. From the temperature-dependent measurements, the activation parameters $\Delta H^{\ddagger}$ and $\Delta S^{\ddagger}$ were found to be 72 ± 3 kJ mol^{-1} and +38 ± 11 J K^{-1} mol^{-1}, respectively. The effect of temperature on pK_{a1} could be roughly estimated using the pK_{a1} values for $[Fe(dapsox)(H_2O)_2]^+$ at two different temperatures, resulting in a very small value of

(13) Andjelkovic, K.; Bacchi, A.; Pelizzi, G.; Jeremic, D.; Ivanović-Burmazović, I. *J. Coord. Chem.* **2002**, *55*, 1385−1392.
(14) van Eldik, R.; Palmer, D. A.; Schmidt, R.; Kelm, H. *Inorg. Chim. Acta* **1981**, *50*, 131−135. (b) van Eldik, R.; Gaede, W.; Wieland, S.; Kraft, J.; Spitzer, M.; Palmer, D. A. *Rev. Sci. Instrum.* **1993**, *64*, 1355−1357.
(15) Zuberbuehler, A. D.; Kaden, T. A. *Talanta* **1982**, *29*, 201−206.
(16) Kitamura, Y.; Itoh, T. *J. Sol. Chem.* **1987**, *16*, 715−725.
(17) Asano, T.; le Noble, W. J. *Chem. Rev.* **1978**, *78*, 469.

Table 1. Kinetic and Activation Parameters for the Reaction of $[Fe(dapsox)(L)_2]^+$ with SCN^- in Different Solvents (L = Solvent or Its Deprotonated Form)[a]

solvent	kinetic parameters	value	$\Delta H^{\ddagger}$ (kJ mol^{-1})	$\Delta S^{\ddagger}$ (J K^{-1} mol^{-1})	$\Delta V^{\ddagger}$ (cm^3 mol^{-1})
MeOH	**step I**				
no acid, 5 °C[b] (25 °C)	k, M^{-1} s^{-1}	601 ± 9 (6370)	87 ± 4	+81 ± 13	+15.0 ± 0.3
acidified, 25 °C	$k_{5(I)}$, M^{-1} s^{-1}	7.17 ± 0.08	76 ± 2	+26 ± 7	+4.5 ± 0.1
	$k_{-5(I)}$, s^{-1}	0.0066 ± 0.0001	76 ± 1	−33 ± 3	−11.4 ± 0.3
	step II				
no acid, 5 °C[b] (25 °C)	k, M^{-1} s^{-1}	4.9 ± 0.2 (60)	80 ± 2	+58 ± 8	+12.0 ± 0.2
acidified, 5 °C (25 °C)	$k_{5(II)}$, M^{-1} s^{-1}	11.1 ± 0.2 (78 ± 2)	63 ± 2	+3 ± 6	+9.2 ± 0.2
EtOH	**step I**				
no acid, 5 °C (25 °C)	$k_{2(I)}$, M^{-1} s^{-1}	1228 ± 19 (6912)	65 ± 1	+45 ± 4	+15.8 ± 0.7
acidified, 25 °C	$k_{5(I)}$, M^{-1} s^{-1}	2.82 ± 0.05	59 ± 2	−37 ± 6	+3.3 ± 0.1
	$k_{-5(I)}$, s^{-1}	0.0025 ± 0.0001	76 ± 3	−40 ± 9	−7.5 ± 0.4
	step II				
no acid, 5 °C (25 °C)	$k_{2(II)}$, M^{-1} s^{-1}	13.2 ± 0.1 (151)	79 ± 2	+61 ± 7	+11.1 ± 0.5
acidified, 5 °C (25 °C)	$k_{5(II)}$, M^{-1} s^{-1}	12.1 ± 0.1 (75 ± 1)	63 ± 1	+2 ± 5	+10.2 ± 0.2
DMSO (25 °C)	$k_{5(I)}$, M^{-1} s^{-1}	0.111 ± 0.004	64 ± 3	−50 ± 9	−1.0 ± 0.5
H_2O (25 °C)	k, M^{-1} s^{-1}				
	step I				
	diaqua[c]	2.19 ± 0.06	62 ± 3	−30 ± 10	−2.5 ± 0.2
	aqua-hydroxo	1172 ± 22 [b]	72 ± 3	+38 ± 11	−3.0 ± 0.1
	step II[c]	21.1 ± 0.5	60 ± 2	−19 ± 6	+8.8 ± 0.3

[a] See the text for the experimental conditions. [b] Reference 12. [c] From ref 9.

Scheme 2

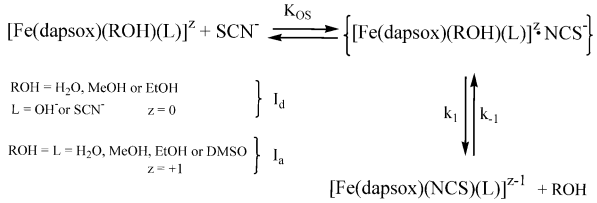

$\Delta H(K_{a1})$ and small negative value of $\Delta S(K_{a1})$. The latter is also in agreement with the above expected small negative value of $\Delta V(K_{a1})$. Thus, the values of $\Delta H^{\ddagger}(k_b)$ and $\Delta S^{\ddagger}(k_b)$ are expected to be similar to the experimentally observed $\Delta H^{\ddagger}$ and $\Delta S^{\ddagger}$. The obtained activation parameters support a dissociative interchange substitution mode for the aqua-hydroxo complex. We have previously observed a curvature in the plot of k_{obs} versus $[SCN^-]$ (under pseudo-first-order conditions using a large excess of SCN^-),[9] and the kinetic data for an I_d mechanism were fitted using the expression for k_{obs} in eq 1 (K_{OS} represents the equilibrium constant for outer-sphere precursor formation; k_1 and k_{-1} are the forward and reverse interchange rate constants, respectively).

$$k_{obs} = k_1 K_{OS}[SCN^-]/(1 + K_{OS}[SCN^-]) + k_{-1} \qquad (1)$$

Since 1 M SCN^- is still far away from the saturation limit of k_{obs} (Figure 4b in ref 9), the observed $\Delta V^{\ddagger}$ in the case of an I_d mechanism is a composite value of $\Delta V^{\ddagger}(k_1)$ and $\Delta V(K_{OS})$. During outer-sphere complex formation, free thiocyanate becomes weakly bound in the precursor complex resulting in a small negative value of $\Delta V(K_{OS})$. Thus, $\Delta V^{\ddagger}(k_1)$ for the rate-determining step in an I_d mechanism is expected to be somewhat more positive than the experimentally obtained value. In terms of a limiting D mechanism, a much more positive value of $\Delta V^{\ddagger}$ would be expected. These arguments favor the operation of an I_d substitution mechanism for the aqua-hydroxo $[Fe(dapsox)(H_2O)(OH)]$ species. It should be noted that water exchange reactions on $[Fe(H_2O)_5OH]^{2+}$[18] and the corresponding complex-formation reactions[19] also follow an I_d mechanism. In comparison, the $\Delta V^{\ddagger}$ value previously obtained for the reaction of [Fe(dapsox)(MeOH)(OMe)] in methanol (viz., +15.0 ± 0.3 cm^3 mol^{-1}) and the value obtained in this work for the reaction in ethanol (viz., +15.5 ± 0.7 cm^3 mol^{-1}) (see Table 1) confirm the operation of a dissociative mechanism for the alcoxo [Fe(dapsox)(ROH)(OR)] species, which can be accounted for by the stronger trans labilization effect of MeO^- and EtO^- than that of OH^-.

Speciation in Alcohol Solutions. It has already been observed that the Fe^{3+} cation exists as $[Fe(MeOH)_5(OMe)]^{2+}$ and $[Fe(EtOH)_5(OEt)]^{2+}$ in methanol and ethanol solutions, respectively.[20] The presence of hydrolyzed cations as the dominant kinetic species accounts for the high rates of solvent exchange and the mechanistic changeover from an associative activation mode for the hexasolvated Fe^{3+} species, to a dissociative one for the deprotonated complexes. It was reported that in anhydrous methanol, even at 5 M acid, it is not possible to fully protonate coordinated MeO^-.[20] Since in aqueous solution our complex is much less acidic (pK_{a1} = 5.78) than aquated Fe^{3+},[9] a similar trend can be expected in alcoholic solutions. Therefore, on addition of triflic acid to alcoholic solutions of the complex, spectral changes similar to those obtained in water, could be observed (spectra b, c, and d in Figure 1), which suggest that protonation of coordinated RO^- takes place. In MeOH, full protonation of the complex can be achieved at 10^{-3} M acid, whereas in EtOH 10^{-2} M acid is required. In comparison, in aqueous

(18) Swaddle, T. W.; Merbach, A. E. *Inorg. Chem.* **1981**, *20*, 4212.
(19) Funahashi, S.; Ishiara, K.; Tanaka, M. *Inorg. Chem.* **1983**, *22*, 2070. (b) Ishiara, K.; Funahashi, S.; Tanaka, M. *Inorg. Chem.* **1983**, *22*, 3589−3592. (c) Grace, M. R.; Swaddle, T. W. *Inorg. Chem.* **1992**, *31*, 4674.
(20) Meyer, F. K.; Monnerat, A. R.; Newman, K. E.; Merbach, A. E. *Inorg. Chem.* **1982**, *21*, 774−778.

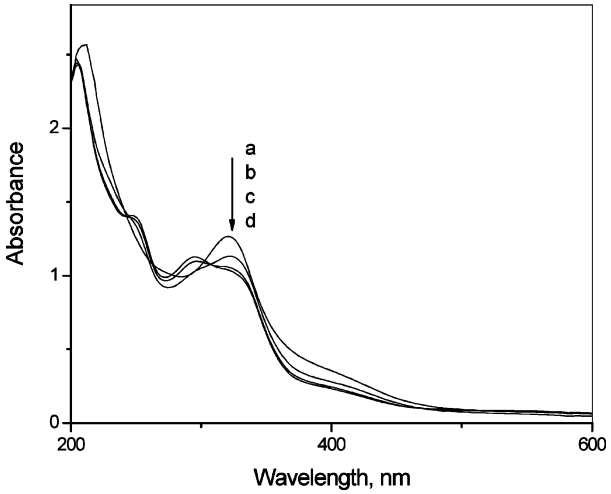

Figure 1. UV−vis spectra of 5×10^{-5} M Fe(III) complex in EtOH: (a) absolute water free EtOH, (b) p.a. grade EtOH, (c) [HOTf] = 10^{-3} M, and (d) [HOTf] = 10^{-2} M.

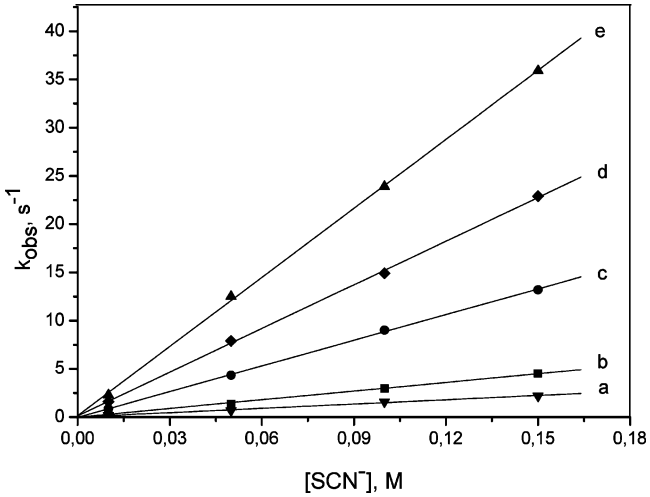

Figure 2. Plots of k_{obs} vs [SCN$^-$] for the second reaction step in EtOH as a function of temperature. Experimental conditions: [Fe(III)] = 5×10^{-5} M; I = 0.3 (LiOTf); T = 5.0 (a), 10.0 (b), 20.0 (c), 25.0 (d), 30.0 °C (e).

solution already at pH ∼5 the diaqua complex is the predominant species. This suggests that coordinated RO^- is a stronger σ-donor than OH^- and a weaker base, such that protonation requires higher acid concentrations. Interestingly, in absolute MeOH and EtOH, the complex has a strong yellow color, and no reaction with SCN^- or any other nucleophiles could be observed. This can be explained in terms of the presence of inert $[Fe(dapsox)(OR)_2]^-$ species in absolute methanol and ethanol solutions, of which the UV−vis spectrum (Figure 1a) is very similar to that of the dihydroxo $[Fe(dapsox)(OH)_2]^-$ species.[9]

Reactions in Ethanol. We have studied the reaction of

$$[Fe(dapsox)(EtOH)(EtO^-)] + SCN^- \rightleftarrows [Fe(dapsox)(NCS)(EtO^-)]^- + EtOH \quad (2)$$

$$[Fe(dapsox)(NCS)(EtO^-)]^- + H^+ \rightleftarrows [Fe(dapsox)(NCS)(EtOH)] \quad (3)$$

$$[Fe(dapsox)(NCS)(EtOH)] + SCN^- \rightleftarrows [Fe(dapsox)(NCS)_2]^- + EtOH \quad (4)$$

our complex (5×10^{-5} M) with SCN^- in an ethanol solution under pseudo-first-order conditions using a large excess of SCN^- ([SCN$^-$] = 0.005−0.15 M) and I = 0.3 M (LiOTf). Kinetic traces clearly showed two subsequent reaction steps over the whole SCN^- concentration range, similar to that observed in MeOH solution (Figure S1, Supporting Information), and they were fitted to a double-exponential function that resulted in k_{obs} values for the first and second reaction steps. Plots of k_{obs} versus [SCN$^-$] (Figure S2) for both reaction steps at 5 °C show a linear increase in k_{obs} with increasing [SCN$^-$] over the whole concentration range without a significant intercept, indicating that there is no reverse solvolysis or parallel reaction. Similar to what we found in aqueous[9] and methanol solutions,[12] the two reaction steps represent the substitution of two axially coordinated solvent molecules by SCN^- as outlined in reactions (2)−(4). The dependence of k_{obs} on [SCN$^-$] for both reactions can be expressed by eq 5, from which the second-order rate constants, k_2, at 5 °C were found to be 1228 ± 19 and 13.2 ± 0.1 M^{-1} s^{-1} for the first and second substitution steps, respectively (Table 1).

$$k_{obs} = k_2[SCN^-] \quad (5)$$

The first reaction is much faster than the second one, similar to that observed for the reactions in MeOH and H_2O. In general the reactivity of the complex in EtOH is higher than that in MeOH and H_2O (Table 1). This is also in agreement with the strong trans effect of the axially coordinated ethoxo group and the high lability of coordinated EtOH in the trans position. The second reaction step is not only thermodynamically more driven in EtOH but also proceeds with the highest rate constant (calculated at 25 °C to be 150 M^{-1} s^{-1}, see Table 1) in comparison to the same step in MeOH and H_2O. It can be accounted for in terms of the weaker donor ability of coordinated EtOH trans to SCN^-.

Activation parameters obtained from the temperature- and pressure-dependent measurements of the first reaction step are summarized in Table 1 (see also Table S2). Plots of k_{obs} versus [SCN$^-$] for the second reaction step as a function of temperature are presented in Figure 2 (see also Table S2), and the corresponding activation parameters are also included in Table 1. Figure 2 clearly illustrates that even for the substitution of the second coordinated solvent molecule there is no intercept. Furthermore, this reaction is thermodynamically strongly driven in ethanol, which is opposite to that found for the reaction in methanol and especially in aqueous solution where the reverse reaction is very prominent even in the case of the first step. The second reaction step was also studied as function of pressure ([SCN$^-$] = 0.05 M at 20 °C), and the results are summarized in Table S2. From a good linear correlation between ln k_{obs} and pressure, the activation volume was found to be $\Delta V^{\ddagger}_{II} = +11.1 \pm 0.5$ cm^3 mol^{-1}. All the activation parameters ($\Delta H^{\ddagger}$, $\Delta S^{\ddagger}$, and $\Delta V^{\ddagger}$, see Table 1) along with the observed trends in the rate constants suggest a dissociative reaction mode for both substitution steps in ethanol, similar to that suggested for

Scheme 3

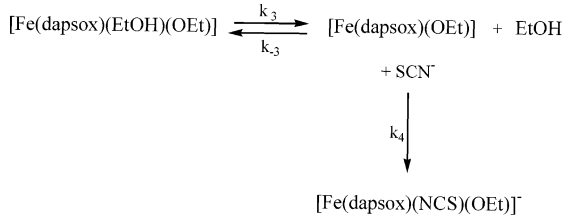

the reaction in methanol. They also suggest the presence of a labile alcoxo [Fe(dapsox)(EtOH)(OEt)] complex in ethanol solution.

Within the concept of a dissociative mechanism, the first step of the investigated reaction can be presented in Scheme 3 with the corresponding expression for k_{obs} given in eq 6.

$$k_{obs} = k_3k_4[SCN^-]/(k_{-3} + k_4[SCN^-]) \qquad (6)$$

Under the selected experimental conditions, $k_4[SCN^-]$ is much smaller than k_{-3} such that eq 6 can be simplified to the form of eq 5, where the overall second-order rate constant k_2 then becomes k_3k_4/k_{-3}. The linear concentration dependence of k_{obs} can easily be understood since thiocyanate is present in a much lower concentration than ethanol to scavenge the six-coordinate intermediate, such that $k_4[SCN^-]$ in eq 6 is negligible in comparison to k_{-3}. The obtained activation volume thus involves contributions from the effect of pressure on the formation of the six-coordinate intermediate ($\Delta V(K_3)$) and on k_4 ($\Delta V^{\ddagger}(k_4)$), since k_2 is a composite value. Although in the present case K_3 ($= k_3/k_{-3}$) and k_4 cannot be kinetically separated, a significantly positive value for $\Delta V(K_3)$ and a negative value for $\Delta V^{\ddagger}(k_4)$ are expected to contribute to the overall value of $\Delta V^{\ddagger}_I = +15.8 \pm 0.7$ cm^3 mol^{-1}.

Coordination of the first SCN^- reduces the acidity of the solvent molecule in the trans position, which results in the rapid protonation of coordinated EtO^- to create a good leaving group (EtOH) and enables the coordination of the second SCN^- ligand. On the basis of the overall positive value of $\Delta V^{\ddagger}_{II}$ ($+11.1 \pm 0.5$ cm^3 mol^{-1}), both a D and an I_d substitution mechanism should be considered. Similar to the first reaction step, in terms of the D mechanism, the observed $\Delta V^{\ddagger}_{II}$ can be interpreted as a composite value, whereas a significantly positive contribution from the dissociation of EtOH and a negative contribution from the formation of the Fe−NCS^- are expected.[21]

An alternative interpretation in terms of a dissociative interchange (I_d) mechanism is based on the idea that [Fe(dapsox)(NCS)(EtOH)] can in the second substitution step form an outer-sphere adduct with SCN^- prior to the substitution reaction similar to that in Scheme 2 (where OR^- is replaced by SCN^-), the difference being that the interchange process is not reversible. Consequently, the expression for k_{obs} can be presented in an equation similar to eq 1, where K_{OS} is the outer-sphere precursor {[Fe(dapsox)(NCS)(EtOH)]·NCS} formation constant and k_1 is the corresponding first-order interchange rate constant. At low SCN^- concentration, $1 + K_{OS}[SCN^-] \approx 1$ and a linear concentration dependence is observed for which the corresponding expression is presented in eq 5, where $k_2 = k_1K_{OS}$ represents the overall second-order rate constant for this reaction step.

This mechanism is similar to that suggested for the second reaction step in aqueous solution,[9] where starting from [Fe(dapsox)(NCS)(H_2O)] the same [Fe(dapsox)$(NCS)_2]^-$ product is formed. The values of $\Delta V^{\ddagger}_{II}$ for the second step in H_2O ($+8.8 \pm 0.3$ cm^3 mol^{-1}) and EtOH ($+11.1 \pm 0.5$ cm^3 mol^{-1}) are also very similar and can be interpreted within the concept of an I_d mechanism.

In terms of the general dissociative nature of the substitution mechanisms proposed above, it is important to note that the higher reactivity of the studied complex in EtOH than in MeOH is in agreement with the higher solvent-exchange rate on Fe^{3+} in EtOH than in MeOH, where the hydrolyzed $[Fe(ROH)_5(OR)]^{2+}$ cations were also found to be the predominant species in alcoholic solutions.[20] Furthermore, it is important to note that solvent exchange on the hydrolyzed $[Fe(ROH)_5(OR)]^{2+}$ cations also occurs via a dissociative mechanism.[20]

Reactions in Acidified Methanol and Ethanol. To study the substitution behavior of the non-hydrolyzed [Fe(dapsox)$(L)_2]^+$ species (L = MeOH and EtOH), we followed the reaction with SCN^- in MeOH and EtOH in the presence of 10^{-3} and 10^{-2} M acid, respectively. The non-hydrolyzed [Fe(dapsox)$(ROH)_2]^+$ species have a much lower reactivity than the hydrolyzed [Fe(dapsox)(ROH)(OR)] complexes, as was also observed in the case of the diaqua and aqua-hydroxo complexes.[9] Therefore, the difference between the rate constants for the two subsequent substitution steps is not that prominent as in the case of nonacidified solutions. Furthermore, the reactivity of [Fe(dapsox)$(ROH)_2]^+$ is lower than that of [Fe(dapsox)(ROH)(NCS)], which results in the slower first and faster second substitution step, in contrast to what has been observed in the absence of added acid. To separate these reaction steps, we performed spectrophotometric titrations in acidified MeOH and EtOH solutions at 25 °C and determined the corresponding equilibrium constants K_1 and K_2 for the binding of the first and the second SCN^-, respectively. To allow equilibration of the solutions, the UV−vis spectra were recorded ca. 30 min after the addition of lower concentrations of SCN^- and 10 min after the addition of higher concentrations of SCN^-. The spectra obtained for the measurements in acidified EtOH and MeOH are presented in Figures 3 and S3, respectively. The absorbances at 468 nm (for titration in acidified EtOH) and 450 nm (for titration in acidified MeOH) versus $[SCN^-]$ were separately fitted for the first and the second equilibrium to eq 7 (Figure S4) and together to eq 8 (inset in Figure 3). The values of A_o and A_∞ represent the absorbance at 0 and 100% formation of the mono and bis(thiocyanato) complexes, respectively, and $\boldsymbol{A}_x$ represents the absorbance at any given thiocyanate concentration. In eq 8, A_o, A_1, and A_2 are the absorbances of [Fe(dapsox)$(ROH)_2]^+$, [Fe(dapsox)(ROH)(NCS)], and

(21) van Eldik, R.; Dücker-Benfer, C.; Thaler, F. *Adv. Inorg. Chem.* **2000**, *49*, 1−58. (b) van Eldik, R.; Hubbard, C. D. In *High-Pressure Chemistry: Synthetic, Mechanistic and Supercritical Applications*; van Eldik, R., Klärner, F.-G., Eds.; Wiley-VCH: Weinheim, Germany, 2002; Chapter 1.

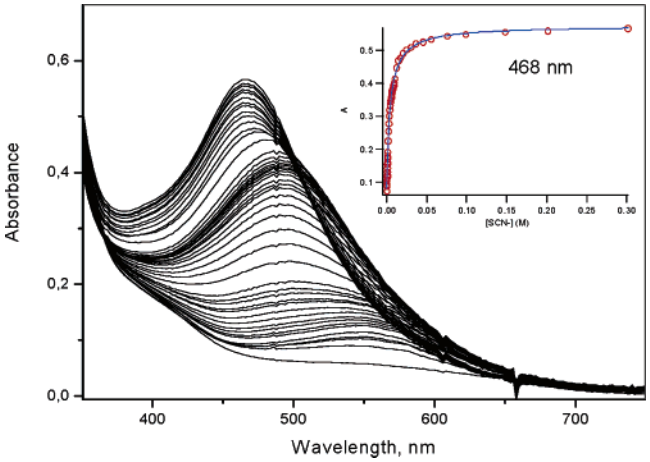

Figure 3. UV−vis spectra recorded during a titration of the Fe(III) complex in acidified EtOH solution with up to 0.3 M SCN^- ([Fe(III)] = 5 × 10^{-5} M, [HOTf] = 10^{-2} M, I = 0.3 (LiOTf), 25.0 °C). Inset. Corresponding changes in absorbance at 468 nm on addition of SCN^- to the Fe(III) complex in acidified EtOH. The solid line is a fit of the data to eq 5 in the text.

$[Fe(dapsox)(NCS)_2]^-$ at a concentration equal to that of the starting complex. Similar values of K_1 and K_2 were obtained by applying these two equations and the average values were found to be $K_1 = 911 \pm 278$ M^{-1}, $K_2 = 126 \pm 32$ M^{-1} and $K_1 = 1654 \pm 210$ M^{-1}, $K_2 = 147 \pm 38$ M^{-1} in acidified EtOH and MeOH solutions, respectively. K_1 and K_2 were also obtained by analyzing the titration spectra in Figures 3 and S3 over the 350−700 nm wavelength range using Specfit/32 global analysis, and the values were found to be $K_1 = 700 \pm 73$ M^{-1}, $K_2 = 170 \pm 41$ M^{-1} and $K_1 = 2080 \pm 220$ M^{-1}, $K_2 = 58 \pm 13$ M^{-1} for acidified EtOH and MeOH solutions, respectively.

$$A_x = A_0 + (A_\infty - A_0)K[SCN^-]/(1 + K[SCN^-]) \quad (7)$$

$$A_x = (A_0 + A_1K_1[SCN^-] + A_2K_1K_2[SCN^-]^2)/(1 + K_1[SCN^-] + K_1K_2[SCN^-]^2) \quad (8)$$

Kinetics of the First Reaction Step. The kinetics of the

$$[Fe(dapsox)(L)_2]^+ + SCN^- \rightleftharpoons [Fe(dapsox)(NCS)(L)] + L \quad (9)$$

$$L = MeOH, EtOH$$

first reaction step (eq 9) were studied using low $[SCN^-]$ (up to 3 mM), which is still a large excess over the complex concentration but low enough that the second reaction step does not interfere. Concentration and temperature dependences are illustrated in Figures 4 and S5 for the acidified EtOH and MeOH solutions, respectively. In both cases the data show good linear plots with significant intercepts within the experimental error limits, suggesting that there are prominent reverse reactions, which is different from the reactions in nonacidified alcohol solutions. From the slopes and the intercepts of the linear plots of k_{obs} versus $[SCN^-]$ the second-order rate constants for the forward reaction, $k_{5(I)}$, and the first-order rate constants for the back reaction, $k_{-5(I)}$, were obtained according to eq 10. The equilibrium constant for the first reaction step can be expressed as $K_1 = k_{5(I)}/k_{-5(I)}$, and the obtained values for the reaction in acidified EtOH (1128 ± 53 M^{-1}) and MeOH (1086 ± 34 M^{-1}) are acceptably close to the thermodynamic values obtained for K_1.

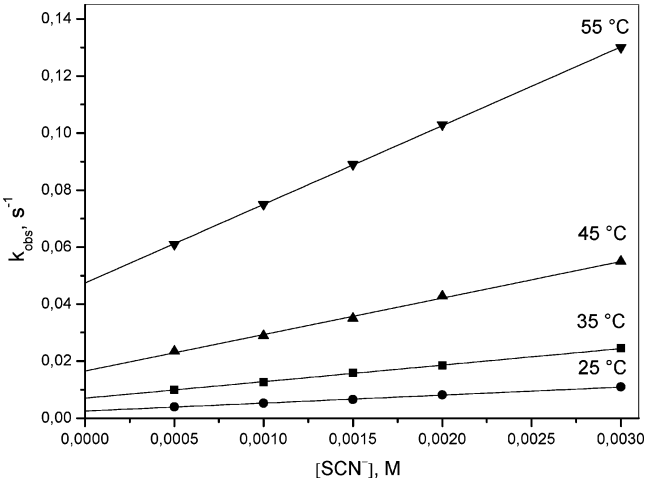

Figure 4. Plots of k_{obs} vs $[SCN^-]$ for the first reaction step in acidified EtOH as a function of temperature. Experimental conditions: [Fe(III)] = 5 × 10^{-5} M, [HOTf] = 10^{-2} M, I = 0.3 (LiOTf).

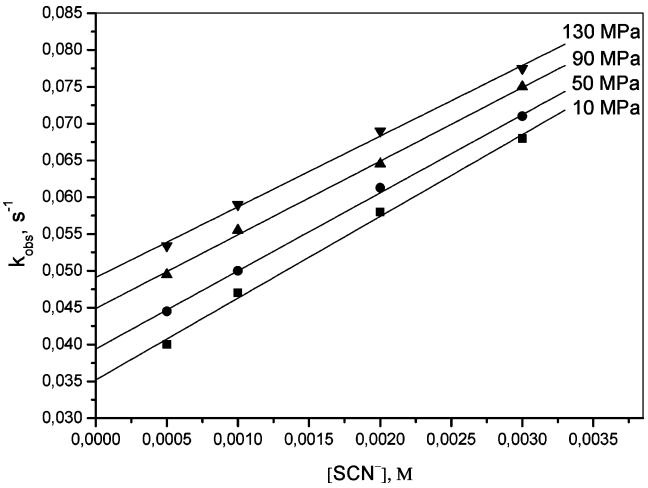

Figure 5. Plots of k_{obs} vs $[SCN^-]$ for the first reaction step in acidified EtOH as a function of pressure. Experimental conditions: [Fe(III)] = 5 × 10^{-5} M, [HOTf] = 10^{-2} M, I = 0.3 (LiOTf), 45 °C.

$$k_{obs} = k_5[SCN^-] + k_{-5} \quad (10)$$

The values of $k_{5(I)}$ and $k_{-5(I)}$ as a function of temperature are given in Tables S3 and S4, and the corresponding activation parameters are summarized in Table 1. As already mentioned, the second-order rate constants for the first substitution step in acidified alcohol solutions are much lower than those in nonacidified alcohols. Also the $\Delta S^{\ddagger}$ values are significantly smaller in the case of the non-hydrolyzed $[Fe(dapsox)(ROH)_2]^+$ species. All this suggests that there is a difference in the substitution mechanism between the $[Fe(dapsox)(ROH)_2]^+$ and [Fe(dapsox)(ROH)(OR)] species.

The first substitution step was also studied as a function of pressure in acidified EtOH and MeOH solutions, and the results are shown in Figures 5 and S6, respectively, from which it follows that good linear plots with significant

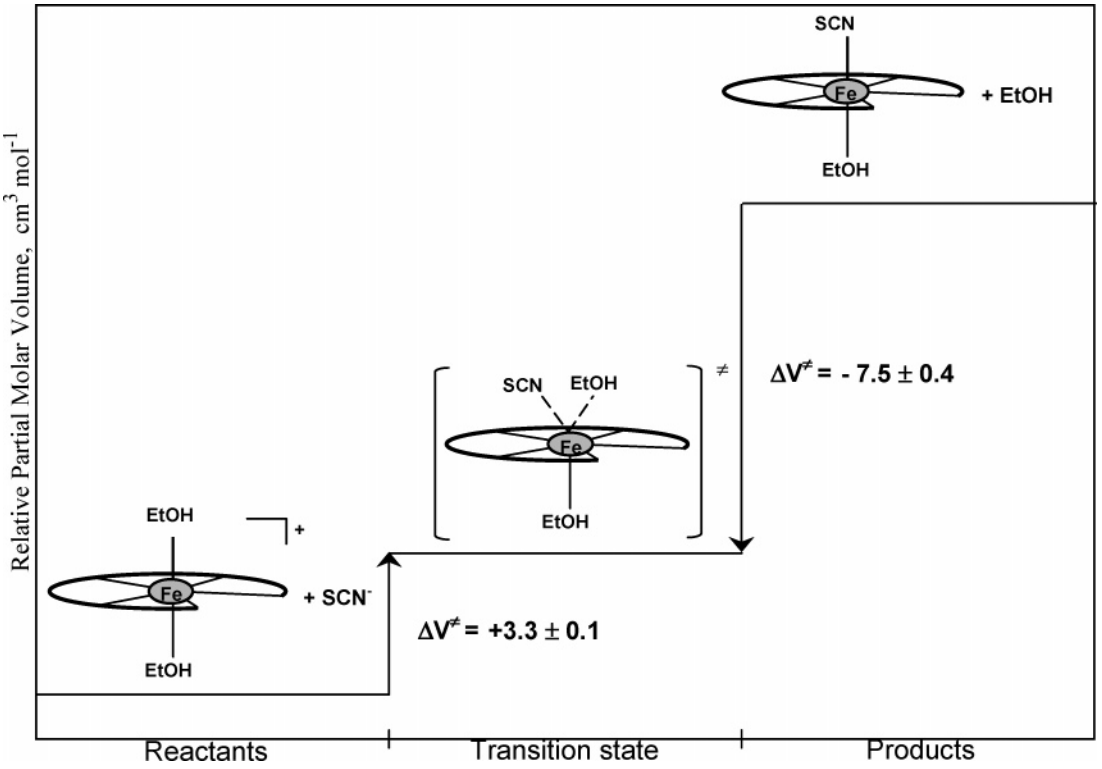

Figure 6. Volume profile for the first reaction step between $[Fe(dapsox)(EtOH)_2]^+$ and SCN^- in acidified EtOH.

intercepts are obtained within the experimental error limits. Interestingly, while the slopes of the plots in Figures 5 and S6 slowly decrease with increasing pressure, the corresponding intercepts increase significantly, suggesting deceleration of the forward and acceleration of the back reaction by increasing pressure. The values of $k_{5(I)}$ and $k_{-5(I)}$ as a function of pressure are given in Tables S3 and S4. Plots of $\ln(k_5)$ and $\ln(k_{-5})$ versus pressure were linear within the error limits, and the corresponding values of $\Delta V^{\ddagger}$ for the forward and the reverse reactions are summarized in Table 1. On the basis of the obtained activation volumes, volume profiles for the first reaction step in acidified EtOH (Figure 6) and MeOH (Figure S7) solutions were constructed. In both solvents a small volume increase accompanies the forward reactions, whereas a somewhat more prominent volume decrease accompanies the reverse solvolysis reactions. However, on the basis of the principle of macroscopic reversibility, the nature of the transition state should be the same for the forward and reverse reaction, and the obtained results can be accounted for in the following way. The forward reaction between $[Fe(dapsox)(ROH)_2]^+$ and SCN^- is accompanied by charge neutralization and results in a decrease in electrostriction (expansion of the surrounding solvent molecules), which is expected to be more prominent in organic solvents than in water. Consequently, the obtained value of $\Delta V^{\ddagger}$ for the forward reaction is more positive than the intrinsic $\Delta V^{\ddagger}$ value for the rate-determining step, which is similar to what was observed for the reaction of $[Fe(dapsox)(H_2O)_2]^+$.[9] The difference is that, in acidified MeOH and EtOH solutions, charge neutralization between $[Fe(dapsox)(ROH)_2]^+$ and the entering SCN^- leads to a more significant decrease in electrostriction of the solvent molecules than in water, which results is a small positive $\Delta V^{\ddagger}$ value that differs from the small negative $\Delta V^{\ddagger}$ observed in water. This, together with the similar second-order rate constants, similar $\Delta H^{\ddagger}$ and $\Delta S^{\ddagger}$ parameters (Table 1), and the existence of significant reverse reactions for the $[Fe(dapsox)(ROH)_2]^+$ and $[Fe(dapsox)(H_2O)_2]^+$ species, suggests the same associative interchange nature of the substitution mechanism for the non-hydrolyzed species of the studied seven-coordinate complex. The proposed mechanism can be presented by Scheme 2, where the rate-determining interchange process (k_1), following precursor formation (K_{OS}), has an associative character. Consequently, eq 1 under the applied experimental conditions (very low SCN^- concentration, $1 + K_{OS}[SCN^-] \approx 1$) becomes eq 10, where $k_{5(I)} = k_1K_{OS}$ represents the overall second-order rate constant for the first reaction step in acidified MeOH and EtOH. Thus, the observed $\Delta V^{\ddagger}$ for the forward reaction is a composite value, i.e., $\Delta V^{\ddagger}(k_{5(I)}) = \Delta V(K_{OS}) + \Delta V^{\ddagger}(k_1)$. Its small positive value results from the sum of a positive contribution from $\Delta V(K_{OS})$ caused by charge neutralization and a small negative contribution from $\Delta V^{\ddagger}(k_1)$ due to an associative interchange mechanism for the rate-determining step. The actual nature of the substitution mechanism is more clearly seen in the activation parameters for the reverse process. Since both reactants are neutral for the solvolysis reaction of [Fe(dapsox)(ROH)(NCS)] in ROH, solvent electrostriction does not contribute significantly and the obtained values of $\Delta V^{\ddagger}$ clearly represent intrinsic volume changes that occur in the rate-determining ligand substitution process. This clearly confirms an associative interchange mechanism.

Kinetics of the Second Reaction Step. The second

$$[Fe(dapsox)(NCS)(S)] + SCN^- \rightleftarrows [Fe(dapsox)(NCS)_2]^- + S \quad (11)$$

$$S = MeOH, EtOH$$

reaction step (eq 11) was studied separately, starting from the mono(thiocyanato) [Fe(dapsox)(ROH)(NCS)] complexes which were prepared by the addition of SCN^- to a 1×10^{-4} M solution of $[Fe(dapsox)(ROH)_2]^+$ in acidified EtOH and MeOH, respectively, so that the final $[SCN^-]$ was 5×10^{-3} M. Such solutions were used in the stopped-flow measurements, where they were mixed with a large excess of SCN^-. The mono(thiocyanato) species have a characteristic red-orange color, different from the orange and yellow of the $[Fe(dapsox)(ROH)_2]^+$ and $[Fe(dapsox)(NCS)_2]$ species (Figures S8), respectively. The second substitution step was studied as a function of $[SCN^-]$ (0.025−0.3 M), temperature (−5 to −25 °C, Figures S9 and S10), and pressure (5−130 MPa), and the data are summarized in Tables 1, S3, and S4. Good linear plots with more significant intercepts at the highest-applied temperature were obtained within the experimental error limits for the reaction in acidified MeOH and EtOH. This behavior can be expressed by the expression given in eq 10, where $k_{5(II)}$ and $k_{-5(II)}$ represent the rate constants for the forward and reverse reactions for the coordination of the second SCN^-. From $K_2 = k_{5(II)}/k_{-5(II)}$, the equilibrium constants for the binding of the second SCN^- in acidified EtOH and MeOH solutions were found to be 250 ± 160 and 65 ± 23 M^{-1}, which is in reasonable agreement with the thermodynamic values obtained for K_2. The values of $k_{5(II)}$ are higher than those of $k_{5(I)}$, confirming the higher reactivity of [Fe(dapsox)(ROH)(NCS)] than $[Fe(dapsox)(ROH)_2]^+$. This is in agreement with the trans effect of SCN^-, which increases the lability of coordinated ROH and, at the same time, causes a changeover in the substitution mechanism and becomes a dissociative interchange process. The postulated I_d mechanism is confirmed by the obtained activation parameters (Table 1), especially by the values of $\Delta V^{\ddagger}$ which are very similar to what was obtained for the second reaction step in nonacidified alcohol and water. Thus, the coordination mechanism of the second SCN^- in acidified MeOH and EtOH can be presented by Scheme 2 and can be discussed as in the case of the nonacidified alcohol solutions (see Reactions in Ethanol).

Reaction in DMSO. To examine the substitution behavior

$$[Fe(dapsox)(DMSO)_2]^+ + SCN^- \rightleftarrows [Fe(dapsox)(NCS)(DMSO)] + DMSO \quad (12)$$

in an aprotic solvent, where hydrolysis does not occur, we studied the reaction of $[Fe(dapsox)(H_2O)_2]ClO_4$ with SCN^- in DMSO as given in eq 12. The IR spectra of the complex in the solid state and in DMSO confirmed that there are no changes in the heptacoodinate structure caused by dissolution in DMSO. The IR spectrum of the complex in DMSO has a new strong band at 955 cm^{-1}, which does not exist in the spectrum of the solid sample. This is a typical ν(S═O) band

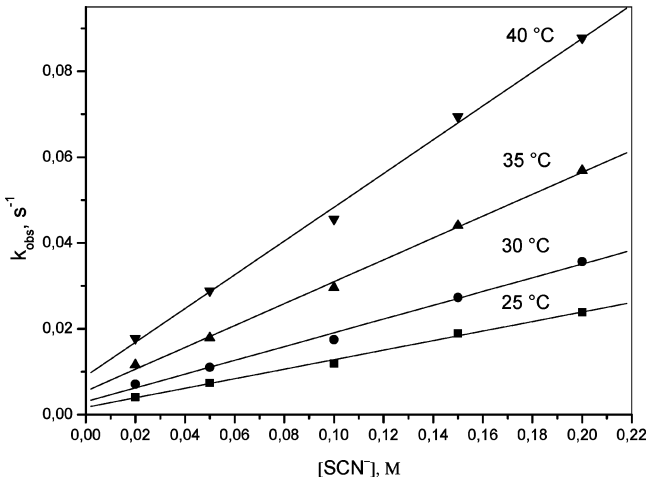

Figure 7. Plots of k_{obs} vs $[SCN^-]$ for the reaction in DMSO as a function of temperature. Experimental conditions: $[Fe(III)] = 5 \times 10^{-5}$ M, $I = 0.3$ M (LiOTf).

for O-coordinated DMSO,[22] which was expected since Fe^{3+} is a hard acid and as such will tend to coordinate to a harder O donor instead of the softer S donor atom. Interestingly, the addition of H_2O (up to ∼5%) to the DMSO complex solution, did not cause any change in the ν(S═O) band, suggesting that this amount of water is not enough to substitute axially coordinated DMSO. Since the complex solubility decreases with increasing water, it was not possible to obtain the IR spectra in DMSO/H_2O mixtures with higher water content. Small amounts of water (up to ∼5%) also did not affect the kinetic measurements. Therefore, detailed kinetic measurements were performed in p.a. grade DMSO without further drying.

The reaction of 5×10^{-5} M complex with an excess of SCN^- ($[SCN^-] = 0.02-0.2$ M, $I = 0.3$ M adjusted with LiOTf) was studied at different temperatures, and the results are shown in Figure 7. Good linear plots with significant intercepts are obtained within the experimental error limits at temperatures up to 40 °C. This behavior can be expressed by eq 10, where k_5 and k_{-5} represent the rate constants for the forward and reverse reactions for the coordination of SCN^-. The values of k_5 and k_{-5} as a function of temperature, along with the corresponding activation parameters are summarized in Table S5. The rate constants for the substitution in DMSO are the lowest in comparison to those obtained in other solvents (Table 1), and in general are quite slow for substitution on Fe(III). This drastic decrease in substitution reactivity upon coordination of DMSO is rather surprising, especially in terms of the seven-coordinate nature of the investigated complex for which high substitution lability would be expected. The values of $\Delta H^{\ddagger}$ and $\Delta S^{\ddagger}$ for the forward reaction (k_5) were found to be 64 ± 3 kJ mol^{-1} and -50 ± 9 J K^{-1} mol^{-1}, respectively, whereas those for the reverse reaction (k_{-5}) were found to be 84 ± 3 kJ mol^{-1} and -15 ± 9 J K^{-1} mol^{-1}, respectively. It should be noted that the intercepts in Figure 7 are subject to large error limits.

(22) Paula, Q. A.; Batista, A. A.; Castellano, E. E.; Ellena, J. *J. Inorg. Biochem.* **2002**, *90*, 144−148. (b) Serli, B.; Zangrando, E.; Gianferrara, T.; Yellowlees, L.; Alessio, E. *Coord. Chem. Rev.* **2003**, *245*, 73−83.

The value of K was determined spectrophotometrically by titrating 5×10^{-5} M $[Fe(dapsox)(H_2O)_2]ClO_4$ ($I = 0.3$ M, LiOTf) with a concentrated stock solution of NaSCN to minimize the effect of dilution at 30 °C. To allow equilibration of the solutions, the UV−vis spectra were recorded ca. 20 min after mixing, and the increase in absorbance at 430 nm was monitored (Figure S11). The solid line in Figure S11 represents a fit of the experimental data to eq 7. The values of K and A_∞ were calculated from a nonlinear least-squares fit of the experimental data. The value of the equilibrium constant K was found to be 45 ± 1 M^{-1}, which is in good agreement with the kinetically obtained value at 30 °C ($k_5/k_{-5} = 53 \pm 13$ M^{-1}).

The pressure-dependent measurements at 40 °C (5×10^{-5} M complex, $[SCN^-] = 0.2$ M, $I = 0.3$ M LiOTf, Table S5) resulted in $\Delta V^{\ddagger} = -1.0 \pm 0.5$ cm^3 mol^{-1}. This suggests the operation of an interchange mechanism for substitution of the axially coordinated DMSO by SCN^- presented in Scheme 2. According to this mechanism, as already discussed above, the pressure effect on k_5, which resulted in $\Delta V^{\ddagger} = -1.0 \pm 0.5$ cm^3 mol^{-1}, is related to the volume change associated with outer-sphere complex formation, ΔV_{OS}, and the activation volume for the interchange process, $\Delta V^{\ddagger}(k_1)$. Since, as a result of charge neutralization, ΔV_{OS} is expected to be positive, $\Delta V^{\ddagger}(k_1)$ should be more negative than -1.0 ± 0.5 cm^3 mol^{-1}. This along with $\Delta S^{\ddagger} = -50 \pm 9$ J K^{-1} mol^{-1} suggests an associative character for the rate-determining interchange process. Thus, the seven-coordinate $[Fe(dapsox)(L)_2]^+$ complexes with non-hydrolyzed H_2O, MeOH, EtOH, and aprotic DMSO solvent molecules as labile axially coordinated ligands undergo substitution of the first solvent molecule by SCN^- according to an associative interchange mechanism (Table 1). The same mechanism has been postulated for solvent exchange on $[Fe(S)_6]^{3+}$, where S = H_2O, MeOH, EtOH, and DMSO[20] and also for the formation of the mono(thiocyanato) $[Fe(H_2O)_5(NCS)]^{2+}$ complex.[19b] This mechanistic similarity is to be expected on the basis of the nature of the metal ion, but since our complex is seven-coordinate with the negatively charged pentadentate chelate, a more dissociative character would in principle be expected. One exception to an I_a mechanism is the formation of $[Fe(DMSO)_5(NCS)]^{2+}$ from $[Fe(DMSO)_6]^{3+}$, in which case a dissociative interchange mechanism has been postulated.[19b] In general it has been anticipated that substitution on Fe(III) should be more dissociative (i.e., less associative) for bulkier solvents.[19b,20] The completely planar and rigid $dapsox^{2-}$ pentadentate chelate in the equatorial plane, generally facilitates easy access of the nucleophiles to the Fe(III) center, without any steric hindrance above and below the pentadentate plane. By way of comparison, four DMSO molecules in the equatorial plane of $[Fe(DMSO)_6]^{3+}$, which can freely rotate around the Fe−O bond, induce a prominent steric hindrance for apical bond formation. Another exception is water exchange on the seven-coordinate $[Fe^{III}(edta)H_2O]^-$ complex, which is characterized by a positive volume of activation and also follows an I_d mechanism.[23]

(23) Schneppensieper, T.; Seibig, S.; Zahl, A.; Tregloan, P.; van Eldik, R. *Inorg. Chem.* **2001**, *40*, 3670−3676.

Conclusions

We have shown that the seven-coordinate $[Fe(dapsox)(H_2O)_2]ClO_4$ complex reacts with SCN^- in the first substitution step according to an associative interchange (I_a) mechanism in acidified methanol, ethanol, and aqueous solutions, as well as in DMSO. The first substitution step proceeds through a dissociative (D) mechanism in methanol and ethanol, but through a dissociative interchange (I_d) mechanism in aqueous solutions at higher pH as a result of the trans effect of alcoxo and hydroxo ligands. Coordination of the second SCN^- always has a dissociative character (I_d or D). These remarkable mechanistic changes and significant differences in the reactivity of the studied complex (Table 1) are not the result of a simple solvent effect but are the result of the presence of different $[Fe(dapsox)(L)_2]^+$ complexes (L = solvent or its deprotonated form) as reactive species. This underlines the role of the axially coordinated solvent molecules in tuning the reactivity and determining the substitution mechanism. In general, non-hydrolyzed $[Fe(dapsox)(L)_2]^+$ species (L = H_2O, MeOH, EtOH, DMSO) react according to an associative mode and much slower than $[Fe(dapsox)(H_2O)(OH)]$, $[Fe(dapsox)(ROH)(OR)]$, and $[Fe(dapsox)(NCS)(L)]$ complexes, which all react in a dissociative way. In terms of the substitution behavior of Fe(III) complexes, such a trend was expected. However, in light of the coordination number seven of the investigated complex, an associative mechanism is an unexpected result. It seems that for the reactivity and substitution behavior of the Fe(III) species, the electronic and steric properties of the chelating ligand and the nature of the axially coordinated solvent molecules are more important than the coordination number.

The results presented here are of fundamental importance for studies on the SOD activity of seven-coordinate Fe(III) complexes. Since the reactions involved are extremely fast, application of DMSO will slow the process and even enable the detection of possible intermediates. On the other hand, to increase the substitution lability and complex reactivity, application of alcoholic solutions will be helpful. It will also be possible to study the role of protons in the reaction with superoxide by using alcoholic solutions at low temperatures, since it was shown that it is possible to protonate and deprotonate the complex under such conditions. Studies on the reaction with superoxide in different solvent systems are presently underway in our laboratories.

Acknowledgment. The authors gratefully acknowledge financial support from the Deutsche Forschungsgemeinschaft through SFB 583 "Redox-active metal complexes" (R.v.E. and I.I.-B.) and the Alexander von Humboldt Foundation (fellowships to I.I.-B. and M.S.A.H.).

Supporting Information Available: Eleven figures and five tables reporting thermodynamic and kinetic data for the substitution reactions in different solvents as a function of thiocyanate concentration, temperature, and pressure. This material is available free of charge via the Internet at http://pubs.acs.org.

IC0514694